HHS Public Access

Author manuscript

Neuroimage. Author manuscript; available in PMC 2017 March 01.

Published in final edited form as:

Neuroimage. 2016 March ; 128: 138–148. doi:10.1016/j.neuroimage.2015.12.056.

Fornix deep brain stimulation circuit effect is dependent on major excitatory transmission via the nucleus accumbens

Erika K. Ross[1,2], **Joo Pyung Kim**[1,3], **Megan L. Settell**[1], **Seong Rok Han**[1,4], **Charles D. Blaha**[1], **Hoon-Ki Min**[1,5,*], and **Kendall H. Lee**[1,5,*]

[1]Department of Neurologic Surgery, Mayo Clinic, Rochester, MN, 55905, USA

[2]Mayo Graduate School, Mayo Clinic, Rochester, MN, 55905, USA

[3]Department of Neurosurgery, Bundang CHA Hospital, CHA University School of Medicine, Seongnam, Korea

[4]Department of Neurosurgery, Ilsan Paik Hospital, College of Medicine, Inje University, Goyang, Republic of Korea

[5]Department of Physiology and Biomedical Engineering, Mayo Clinic, Rochester, MN, 55905, USA

Abstract

Introduction—Deep brain stimulation (DBS) is a circuit-based treatment shown to relieve symptoms from multiple neurologic and neuropsychiatric disorders. In order to treat the memory deficit associated with Alzheimer's disease (AD), several clinical trials have tested the efficacy of DBS near the fornix. Early results from these studies indicated that patients who received fornix DBS experienced an improvement in memory and quality of life, yet the mechanisms behind this effect remain controversial. It is known that transmission between the medial limbic and corticolimbic circuits plays an integral role in declarative memory, and dysfunction at the circuit level results in various forms of dementia, including AD. Here, we aimed to determine the potential underlying mechanism of fornix DBS by examining the functional circuitry and brain structures engaged by fornix DBS.

Methods—A multimodal approach was employed to examine global and local temporal changes that occur in an anesthetized swine model of fornix DBS. Changes in global functional activity were measured by functional MRI (fMRI), and local neurochemical changes were monitored by fast scan cyclic voltammetry (FSCV) during electrical stimulation of the fornix. Additionally, intracranial microinfusions into the nucleus accumbens (NAc) were performed to investigate the global activity changes that occur with dopamine and glutamate receptor-specific antagonism.

[*]Corresponding authors; Kendall H. Lee (lee.kendall@mayo.edu) and Hoon-Ki Min (min.paul@mayo.edu); Mayo Clinic, 200 First Street SW Rochester, MN 55905, USA.

Financial Disclosure: The authors declare no competing financial interests.

Results—Hemodynamic responses in both medial limbic and corticolimbic circuits measured by fMRI were induced by fornix DBS. Additionally, fornix DBS resulted in increases in dopamine oxidation current (corresponding to dopamine efflux) monitored by FSCV in the NAc. Finally, fornix DBS-evoked hemodynamic responses in the amygdala and hippocampus decreased following dopamine and glutamate receptor antagonism in the NAc.

Conclusions—The present findings suggest that fornix DBS modulates dopamine release on presynaptic dopaminergic terminals in the NAc, involving excitatory glutamatergic input, and that the medial limbic and corticolimbic circuits interact in a functional loop.

Keywords

deep brain stimulation; fornix; nucleus accumbens; functional magnetic resonance imaging; fast scan cyclic voltammetry; dopamine

Introduction

Deep brain stimulation (DBS) is a neurosurgical treatment for various neurologic and neuropsychiatric disorders, including Parkinson's disease, dystonia, major depression, and obsessive-compulsive disorder (Benabid, 2003; Benabid et al., 1991; Greene, 2005; Lozano et al., 2012). Recently, DBS has been applied within the medial limbic circuit (Papez circuit), to address memory deficits associated with dementia (Laxton et al., 2010; Ponce et al., 2015; Smith et al., 2012; Suthana et al., 2012). These early clinical studies indicated patient improvement in cognition, memory, and quality of life, and suggested that neural activity in memory-related circuitry might underlie this effect (Hardenacke et al., 2013; Lee et al., 2013).

The medial limbic circuit is one of the major pathways primarily involved in the cortical control of emotions and memory function (Rajmohan and Mohandas, 2007). This circuit includes the hippocampus (HP), fornix, mammillary body, anterior nucleus of the thalamus, cingulate cortex, parahippocampal gyrus, and entorhinal cortex (Mesulam, 2000). Within this circuit, the fornix is a major candidate brain target for DBS to treat memory impairment (Hescham et al., 2013; Laxton and Lozano, 2013). Specifically, in Alzheimer's disease (AD), it is proposed that fornix DBS influences memory recall by enhancing activity across distinct nodes involved in memory retrieval (Lee et al., 2013). One possible issue with fornix DBS arises from the diverse axons that travel through the fornix and terminate in distinct structures, including medial limbic and corticolimbic circuit components. The fornix has major input and output pathways from the HP and medial temporal lobe as well as the HP to the nucleus accumbens (NAc) that have known involvement in an array of cognitive processes (Kahn and Shohamy, 2013; Saint Marie et al., 2010). Although fornix DBS likely involves a wide range of axonal fiber effects, characterizing the electrical stimulation-induced response on neuronal communication beyond a few synapses is extremely challenging.

In place of a modular paradigm that views brain areas as independent processors, it is now accepted that dynamic functional connectivity among distributed neural nodes underlies many of the more complex neural functions (Bressler and Menon, 2010; McIntosh, 1999;

Sporns, 2014). Communication between regions of the medial limbic and corticolimbic circuits, including the HP, NAc, amygdala (AM), and prefrontal cortex (PFC), are known to be critical for memory consolidation and retrieval (Badre et al., 2014; Carr et al., 2011; Hamann et al., 1999; Horner et al., 2015; Lisman and Grace, 2005; Schedlbauer et al., 2014). The ventral striatum in particular, which includes the NAc, is involved in cognitive control during memory retrieval (Scimeca and Badre, 2012; Speer et al., 2014). Moreover, functional MRI (fMRI) studies have shown that AD patients show decreased resting state activity in HP, PFC, and increased ventral striatum activity compared to age-matched controls (Buckner et al., 2005; Greicius et al., 2004; Zhou and Seeley, 2014). Together, these observations suggest that the interconnected circuits play a distinct role in memory consolidation and retrieval, and are affected during memory dysfunction in AD.

In order to investigate the global circuit involvement during DBS, we have developed a technique that combines DBS and functional MRI (fMRI), as a means of tracing brain circuitry and testing the modulatory effects of electrical stimulation on a neuronal network (Knight et al., 2015; Min et al., 2014; Min et al., 2012). Using this setup, we aimed to trace fornix DBS-induced global neural activity. Here, we measured the global blood oxygen level-dependent (BOLD) changes following different pharmacological manipulations and local dopaminergic neurotransmission in the NAc to determine the functional connectivity between the medial limbic and corticolimbic circuits following fornix DBS.

Experimental Procedures

Experimental Overview

Global and local changes associated with fornix stimulation were measured using three distinct experimental paradigms: 1) global hemodynamic changes using fMRI during fornix stimulation, 2) local neurochemical changes with fornix stimulation, and 3) global changes using fMRI pre- and post-NAc intracranial drug microinfusion. All experiments began with stimulating lead implantation in the fornix, followed by fMRI and intracranial drug microinfusions or carbon fiber microelectrode implantation and FSCV (Figure 1A). In order to accurately and consistently implant the DBS electrode lead while minimizing inter-subject variability, high-resolution image-based targeting was performed as previously described (Min et al., 2012; Kim et al., 2013). The DBS electrode was implanted anterior and parallel to the medial portion of the fornix, in order to avoid penetrating the tract, as damage to these fibers is known to cause memory deficits (Laxton et al., 2010; Tsivilis et al., 2008; Vann et al., 2009; Wilson et al., 2008). To confirm that the target matched the final location of the electrode, post-surgical CT scans were co-registered with the pre-surgical magnetization prepared rapid acquisition gradient echo (MPRAGE) scan (Figure 1C). For each subject, DBS lead contacts one and two were marked on the sagittal plane of the swine brain atlas (Figure 1C) (Felix et al., 1999).

Subjects

All study procedures were performed in accordance with the National Institutes of Health Guidelines for Animal Research and approved by Mayo Clinic Institutional Animal Care and Use Committee. The subject group consisted of 17 normal healthy domestic swine

(30±3kg). For all experiments, subjects received high frequency electrical stimulation utilizing the parameters: biphasic 3, 5, or 7 V pulses at 130 Hz and pulse width of 150 μsec (A-M system optical-isolated pulse stimulator Model 12100, Sequim, WA, USA).

Stereotactic Surgery

DBS electrode targeting and implantation was performed with an MR image-guided Leksell stereotactic targeting system (Elekta Inc., Stockholm, Sweden) modified for large animals (Min et al., 2012; Kim et al., 2013). A 3 Tesla MR scanner (General Electric Healthcare, Wakasha, WI; Signa HDx, 16× software) with a custom four-channel transmit-receive radiofrequency coil was used for preoperative anatomical imaging. 3D MPRAGE images were used for MR image-based targeting with swine brain atlas and COMPASS navigational software (modified for large animals) to determine the Leksell coordinates for stimulation target (Felix et al., 1999; Saikali et al., 2010; Shon et al., 2010).

Sedation was maintained with 1.5-3% isoflurane during surgery and 1.5-1.75% isoflurane during the fMRI and NAc dopamine recording experiments. Vital signs were continuously monitored throughout the procedures. Upon sedation, subjects were implanted with a quadripolar (contacts labeled 0, 1, 2, and 3) DBS electrode (Model 3389, Medtronic,Inc.). The electrode was positioned 2 mm anterior and parallel to the fornix unilaterally based on the brain atlas and anatomical landmarks (e.g., optic chiasm and mammillary bodies) to avoid a lesion in the white matter fibers of the fornix (Figure 1B) (Laxton et al., 2010). The location of the electrode was confirmed through a post-surgical computer tomography (CT) (dual source Somatom definition, Siemens AG) scan (image resolution 0.6 × 0.6 × 0.6 mm) which was co-registered using a 6-parameter rigid-body transformation with the pre-surgical MPRAGE scan (Figure 1C) (FSL, FM-RIB Analysis group) (Cho et al., 2010; Smith et al., 2004; Starr et al., 2002).

fMRI Acquisition

Functional imaging was acquired with a custom six channel transmit-receive radiofrequency coil using gradient echo-echo planar imaging (GRE-EPI): repetition time (TR) = 3000 ms; echo time = 34.1 ms; flip angle = 90°; frequency direction, R/L; field of view = 15 cm × 15 cm; matrix size = 64 × 64; axial slices 2.4 mm thick with no gap; slice number= 32; spatial resolution = 2.34 × 2.34 × 2.4 mm; scan duration = 390 sec; 130 scans; integrated spatial spectral pulse was used for fat suppression. For anatomical registration, an additional single scan (GRE-EPI) was acquired in the identical orientation as the fMRI. After 5 volumes of discarded acquisitions to allow for scanner equilibrium, electrical stimulation was applied in a block paradigm with five six-sec-stimulation epochs interspersed with 1 min of rest, with 10 min of rest between scans.

fMRI Post-Processing and General Linear Model (GLM) Analysis

A standard pre-processing sequence, including slice scan time correction, three dimensional motion correction, temporal filtering (High-pass: Fourier basis set = 5 cycles, and low-pass: Gaussian filter, full width at half-maximum = 3.1 sec), and spatial smoothing (Gaussian filter with full width at half-maximum = 1.1 pixels) was applied to each data set (Brain Innovation, BrainVoyager QX, Netherlands). Double-gamma hemodynamic response

function (onset = 6 sec, time to response peak = 11 sec, time to undershoot peak = 21 sec, response undershoot ratio = 3) correlated voxel-wise BOLD signal changes with the given stimulus protocol were calculated by linear regression. For group analysis, the fMRI data were co-registered to the anatomical 3D MPRAGE images using acquired 2D GRE-EPI images and 3D swine brain atlas, as previously described (Min et al., 2012; Kim et al., 2013).

Region of Interest (ROI) Definition

The total voxel size of significant change was measured (mm^3), and discrete clusters were determined by anatomically defined brain structures in the 3D swine brain atlas as the result of a multi-subject general linearized model (GLM). To correct for multiple comparisons and exclude false positive and negative voxels, only voxels with significance level less than the False Discovery Rate (FDR<0.001) were considered. In addition to and separate from the FDR, we applied the more stringent Bonferroni correction ($p<0.001$) to the original data (Table 1). The measure of interest was the maximum or minimum event-related BOLD response (e.g., the minimum BOLD signal/5 volume average of baseline BOLD signal). This BOLD signal intensity change (%), representing minimum or maximum response intensities within each cluster, was labeled “BOLD % change” (mean±SEM).

Stereotactic Intracranial Receptor Antagonist Infusion

For unilateral drug microinfusions, the NAc was targeted from the pre-operative MP-RAGE image. A 100 μl syringe and small hub removable needle (23 gauge, 2.1 in) were used for all drug infusions (Hamilton CO, Reno, NV, USA). A 40 μl volume of vehicle (n=3), the broad-spectrum ionotropic glutamate receptor antagonist kynurenic acid (10 mg/mL; n=3), or the D1/D2 dopamine receptor antagonist α-flupenthixol (30 mg/mL; n=3) was injected at a constant rate of 0.3 μl/min into the NAc. Vehicle consisted of one drop of sodium hydroxide (0.1 M) in PBS, final pH adjusted to 7.0 with hydrochloric acid (0.1 M). Kynurenic acid was dissolved in one drop of sodium hydroxide (0.1 M) in PBS, with final pH adjusted to 7.0 with hydrochloric acid (0.1 M). α-Flupenthixol was dissolved in PBS, with final pH adjusted to 7.0. Microinfusions were performed using the Ultra micro pump with SYS-Micro4 controller (World Precision Instruments, Inc., Sarasota, FL, USA) mounted to a Kopf stereotactic carrier adapted to the head frame. The Hamilton syringe needle was left in place for 10 min post-infusion. α-Flupenthixol and kynurenic acid were purchased from Sigma-Aldrich (St. Louis, MO, USA).

fMRI scans were performed 1 h after drug infusion. To confirm drug diffusion was contained in the NAc, the contrast agent Magnevist (gadopentetate dimeglumine) was injected in a similar manner and volume as drug or vehicle and anatomical MPRAGE scan was performed (Figure 1B). Changes in DBS-evoked BOLD increases (FDR, $p<0.001$) pre- and post-infusion were evaluated by calculating the difference in the maximum BOLD percent change between pre- and post-drug injection within a single subject. Maximum BOLD percent change was then compared between groups. In addition to and separate from the FDR, we applied the more stringent Bonferroni correction ($p<0.001$) to the original data. The brain areas that survived Bonferroni correction are listed in Table 2.

Fast Scan Cyclic Voltammetry (FSCV)

Electrochemical recordings were made using conventional carbon fiber microelectrodes, fabricated as previously described (Chang et al., 2012). Electrodes had an exposed diameter of 7 μm and length of 50–100 μm. The tip of the fiber was placed in the NAc using MPRAGE anatomical imaging. FSCV recording was performed using the wireless instantaneous neurotransmitter concentration sensor system (Bledsoe et al., 2009; Shon et al., 2010). The carbon fiber microelectrode was held at −0.4 V, and triangular waveforms (−0.4 to 1.5 V versus Ag/AgCl at 400 V/sec) were applied at 10 Hz. Background subtracted cyclic voltammogram currents were obtained by subtracting the average of 10 voltammograms obtained prior to electrical stimulation (3 V, 130 Hz, 150 μs for 6 sec) from each voltammogram obtained after stimulation. The time course of changes in dopamine efflux in response to fornix DBS was determined by plotting changes in peak dopamine oxidation currents versus time. For FSCV experiments, a 6 sec stimulation was followed by a 5 min rest period.

Results

Fornix stimulation DBS results in BOLD increases within the medial limbic and corticolimbic circuits

In order to examine global functional connectivity, BOLD changes were measured following direct electrical stimulation of the fornix. With fornix stimulation (3 V), BOLD signal intensity increases were observed in areas of the medial limbic circuit, including the ipsilateral HP, fornix, entorhinal cortex, parahippocampal gyrus, and the mammillary body, as well as hippocampal circuit structures, including the inferior temporal gyrus (ITG) as measured by BOLD percent change (FDR, $p<0.001$). There were additional BOLD increases within many structures of the corticolimbic circuit following fornix stimulation. Significant BOLD increases were observed in the NAc, PFC, AM, ventral tegmental area (VTA), substantia nigra, insular cortex, and dorsal anterior cingulate (Figure 2A). Stimulation amplitude effect is shown in figure 2B, highlighting the PFC, NAc, AM, and HP. Finally, total voxel size of significant change was measured (mm^3), and compared as a function of stimulation amplitude, revealing that cluster size increased in the PFC, NAc, HP and AM (Table 1). Additional structures connecting to the medial limbic structures showed increased BOLD response, including the hypothalamus and primary somatosensory cortex. Increased stimulation amplitude also resulted in increased cluster size in additional brain structures, including many contralateral structures with increased stimulation amplitude (Table 1 & Supplementary Figure 1).

Characterization of NAc dopamine efflux in response to fornix electrical stimulation

Dopamine release within the NAc has been linked to a positive BOLD response in the NAc (Knutson and Gibbs, 2007). Although the exact role that dopamine release has on BOLD response is unclear, it has been shown to have a direct effect on local cortical blood flow (Krimer et al., 1998; Zaldivar et al., 2014). Upon observing a dopaminergic corticolimbic involvement following fornix electrical stimulation, local real-time dopaminergic transmission in the NAc, associated with indirect BOLD changes, was assessed using FSCV. As shown in the representative pseudo-color plot in figure 3A, fornix stimulation at 3 V

induced a triphasic change in the dopamine signature oxidation current with a stimulation-time locked peak increase within 8 sec after the initiation of stimulation, followed by a peak decrease below pre-stimulation baseline within 24 sec, and thereafter a second peak increase within 68 sec returning to pre-stimulation baseline levels by 132 sec. The recorded cyclic voltammogram exhibited an oxidation peak at +0.6 V and a reduction peak -0.2 V, consistent with the oxidation of dopamine and reduction of the electroformed dopamine ortho-quinone, respectively (Figure 3B). Figure 3C shows the current vs. time plot in three subjects (Mean±SEM).

NAc intracranial dopamine and glutamate receptor antagonist microinfusions change fornix stimulation-evoked BOLD response

Given the ability of fornix stimulation to modulate dopaminergic transmission in the NAc, global BOLD changes were determined following pharmacological blockade of dopamine and glutamate receptors in the NAc to determine the functional connectivity between the medial limbic and corticolimbic circuits (Kim et al., 2013; Min et al., 2012). Rather than investigating differential dopamine D1-like and D2-like receptor actions in the NAc the D1/D2 dopamine receptor antagonist α-flupenthixol was employed. As shown in Figure 4B, intra-NAc microinfusion of α-flupenthixol (n=3) resulted in BOLD decrease in the HP and AM, as compared to changes following vehicle microinfusions (Figure 4A). These attenuating effects of intra-NAc infusions of α-flupenthixol were decreased in comparison within the NAc and PFC (Figure 4D). Cluster size analysis revealed that α-flupenthixol caused a global decrease in regions of the corticolimbic and medial limbic circuits, whereas vehicle microinfusion resulted in little change compared to pre-infusion (Table 2).

Dopamine release in the NAc regulates the way that GABAergic medium spiny neurons (MSNs) respond to limbic (AM and HP) and cortical (PFC) excitatory glutamatergic inputs (Floresco, 2015). As shown in figure 4C, intra-NAc microinfusions of the broad-spectrum ionotropic glutamate receptor antagonist kynurenic acid (n=3) resulted in a similar decrease in the BOLD signal in the AM, and in the PFC and HC, as compared to changes following vehicle microinfusion (Figure 4D). The BOLD time course pre- and post-drug injection is summarized in supplementary figure 2. Cluster size analysis revealed that kynurenic acid injection resulted in specific cluster size decreases in regions of the corticolimbic and medial limbic circuits, yet did not change the response in the ITG (Table 2). Microinfusion of the MRI contrast agent Magnevist, in a similar manner and volume as drug or vehicle prior to anatomical MPRAGE scan, confirmed drug diffusion was contained within the NAc (Figure 1B).

Discussion

The goal of the present study was to examine the global circuit involvement following fornix DBS in an anesthetized large animal model mimicking exploratory therapeutic application of DBS in AD patients, and the role of the NAc in propagating the stimulation-induced global changes in the brain. Our fMRI studies revealed that fornix stimulation induced global BOLD increases in medial limbic and corticolimbic circuits. In addition, using the real-time neurotransmitter monitoring technique of FSCV, fornix stimulation was

found to evoke a triphasic change in dopamine oxidation current (corresponding to dopamine efflux) in the NAc. Additional fMRI studies following intracranial microinfusion indicated that dopamine or glutamate receptor antagonism in the NAc attenuated fornix stimulation-induced activity in the HP and AM. These findings are consistent with the hypothesis that fornix DBS drives medial and corticolimbic circuit interaction in a functional loop, involving dopaminergic and glutamatergic transmission through the NAc.

Fornix stimulation drives BOLD increases in medial limbic and corticolimbic circuit structures

Our results indicated that fornix stimulation induced a positive BOLD response throughout many integral structures within the medial limbic and corticolimbic circuits. There has been a great deal of basic and clinical work aimed at understanding these circuits and mechanisms by which they interact, providing a wealth of information on the contribution to behavior and disease (Adcock et al., 2006; Berke and Hyman, 2000; Goto and Grace, 2008; Kelley, 2004; Luthi and Luscher, 2014; Sesack and Grace, 2010), yet there are few studies investigating the global circuit involvement. Fundamental work investigating the role of this circuitry in memory has established that autobiographical memory depends on medial limbic circuit structures, is centered around the HP, and that normal aging affects engagement of the HP during memory recall (Maguire and Frith, 2003; Squire, 1992, 2004). Additional investigation into disease-state alterations has revealed that memory deficit, specifically in AD, is directly related to decreased hippocampal network connectivity (Buckner et al., 2005; Greicius et al., 2004; Nestor et al., 2006; Zhou and Seeley, 2014). Moreover, AD patients show increased pathology in regions of this circuitry, including the HP, ventral striatum, and the PFC (Arnold et al., 1991; Geula, 1998; Hyman et al., 1984; Selden et al., 1994). As such, our results indicate that fornix DBS increases activity within these areas, which could help to decipher findings from fornix DBS clinical trials. Results from these studies indicated that bilateral fornix DBS resulted in increased glucose metabolism in structures of the medial limbic and corticolimbic circuits after one year compared to baseline, which correlated with improvements in memory, cognition and quality of life (Laxton et al., 2010). Additionally, two patients in this study experienced hippocampal volume increase, possibly resulting from increased activity within the HP following fornix DBS (Sankar et al., 2014). Indeed, recent studies suggest that electrical stimulation of the brain may promote neurogenesis and pro-survival effects on existing cells in the HP (Hardenacke et al., 2013).

More recently, convergence of information from the medial limbic circuit and several structures within the corticolimbic circuit are thought to play a critical role in memory recall that is dependent on motivationally important events (Lisman et al., 2011; Shohamy and Adcock, 2010). The PFC, AM, and NAc, in particular, have been shown to contribute to cognitive control of memory consolidation and recall (Badre et al., 2014; Hamann et al., 1999; Lisman and Grace, 2005; Schedlbauer et al., 2014; Scimeca and Badre, 2012; Speer et al., 2014). In the present study fornix DBS resulted in increased BOLD response within the NAc, PFC, and AM, and this result may help to explain the improvement in memory recall as well as play a role in the observed improvements in cognition with fornix DBS.

Increases in BOLD response were also observed in structures outside of the medial limbic and corticolimbic circuits, including the prepyriform and somatosensory cortices. Projections between the HP and the prepyriform cortex have been implicated in AD and pathology within the prepyriform has been shown in AD patients (Kawaguchi and Simon, 1997; Reyes et al., 1987). Additionally, the somatosensory cortex has been shown to be vulnerable to degeneration early in the progression of AD, although not as susceptible as areas in the temporal lobe and frontal and parietal association areas (Geula, 1998). Together, these data point to a potential mechanism underlying clinically effective fornix DBS in AD. We recognize that our data are an average of the 5 responses following stimulation and that attenuation and potentiation may occur through the course of the scan. We would need to conduct further experiments to characterize these effects.

Dopaminergic neurotransmission in NAc in response to fornix stimulation

Communication between the HP and the NAc is critical for memory consolidation and retrieval (Adcock et al., 2006; Kahn and Shohamy, 2013; Lisman and Grace, 2005; Wittmann et al., 2005). Increase of NAc cellular activity following stimulation of the fornix-fimbria or ventral subiculum in rat (Boeijinga et al., 1993; Boeijinga et al., 1990; Yang and Mogenson, 1984, 1985) and cat (Lopes da Silva et al., 1984) have been previously reported. These studies, in combination with previous fMRI studies in rats showing BOLD increase in NAc following main hippocampal afferent pathway stimulation, are in agreement with the present data (Helbing et al., 2013; Krautwald et al., 2015). The HP, VTA, and NAc have high intrinsic functional interconnectivity, which provides the framework for this interplay (Kahn and Shohamy, 2013). Dopaminergic projections from the VTA to the NAc are strongly influenced by medial limbic circuit structures, and glutamatergic afferent projections from the HP to the NAc have a strong resultant excitatory effect on dopamine synaptic activity (Floresco et al., 2001). Based on this connectivity, functional connections between medial limbic and corticolimbic circuits provide a framework for known dopaminergic and glutamatergic interactions. Neurochemical and behavioral evidence suggests that dopaminergic and glutamatergic synaptic convergence in the NAc provides information that dictates cognitive function involved in memory, learning, attention, and motivation (Berke and Hyman, 2000; Day et al., 2007; Flagel et al., 2011; Kelley, 2004; Pennartz et al., 2011).

Given the observation of increased BOLD changes in NAc, AM, PFC, and the HP, specific neurotransmitters involved at the level of the NAc were investigated following fornix DBS. We found an initial increase then decrease followed by a relatively long and latent increase in dopamine efflux in the NAc following fornix stimulation. The precise neural circuitry involved in the modulation of NAc dopamine release by fornix stimulation was not definitively determined in the present study. It is important to note that our fMRI experiments were cyclical, with a 6 sec stimulation period followed by 60 sec rest, whereas the FSCV measurements involved a single stimulation period. These stimulation pattern differences could have resulted in qualitatively and/or quantitatively altered dopamine-release kinetics, which were not addressed here.

Previous studies in rodents have provided the foundation to address the potential pathways involved in DA release in the NAc following fornix stimulation. HP stimulation-evoked dopamine efflux is, at least in part, mediated by ionotropic glutamate receptors within the NAc (Blaha et al., 1997). The major cell population in the NAc is GABAergic MSNs, with predominant extrinsic innervation from excitatory glutamatergic projections from the HP, PFC, and AM (Friedman et al., 2002; Kelley and Domesick, 1982; Sesack and Grace, 2010). There are several pathways through which fornix stimulation may modulate dopaminergic activity in the NAc. The first is a direct monosynaptic pathway that involves glutamatergic efferent fibers that project from the ventral subiculum of the HP, through the fornix, and into the NAc (Kelley and Domesick, 1982), where they synapse on MSNs in close apposition with VTA projection terminals (Totterdell and Smith, 1989). HP afferents to the NAc via the fornix are necessary for NAc neurons to enter an active state (O'Donnell and Grace, 1995). In addition, there are at least three distinct polysynaptic pathways that provide the neuronal framework for dopamine release within the NAc following fornix stimulation. The first involves ventral HP glutamatergic projections through the fornix to the NAc to activate GABAergic projections to the ventral pallidum to inhibit pallidal GABAergic input to VTA dopamine neurons (disinhibition) (Floresco et al., 2001; Valenti et al., 2011), while the second involves dorsal HP glutamatergic projections to GABAergic neurons in the lateral septum that, in turn, project to GABAergic interneurons in the VTA to also disinhibit VTA dopamine neurons (Luo et al., 2011; Rossato et al., 2009). Finally, a third involves an excitatory loop with glutamatergic projections from the HP through the fornix to the PFC that, in turn, send glutamatergic projections to dopaminergic cells in the VTA (Saunders and Aggleton, 2007; Rossato et al., 2009; Luo et al., 2011).

Electrical stimulation (100 Hz) in the ventral subiculum of the HP has previously been shown to evoke dopamine release in the NAc in rats, beginning with an initial transient increase in the dopamine signal above baseline, followed by an immediate decrease below baseline, and thereafter by a prolonged increase in the dopamine signal above baseline, which were all blocked by transection of the fimbria-fornix (Blaha et al., 1997). The observation that increases in dopamine cell firing is accompanied by an increase in dopamine efflux in the NAc suggests that projections from the ventral subiculum of the HP may modulate NAc dopamine release via direct changes in dopamine neuron activity both at the terminal and cell body level (Floresco et al., 2003; Blaha et al., 1997; Legault et al., 2000). Recent research has shown that neurons projecting to the NAc are neurochemically diverse, and include not only projections that release dopamine, but also glutamate and GABA (Stuber et al., 2010; Zhang et al., 2015). This suggests that this mechanism may be more complicated and may involve more comprehensive circuit interactions. Based on these findings, we next sought to further determine the connectivity and the role of glutamate and dopamine receptors within the NAc mediating fornix stimulation.

Intracranial NAc dopamine and glutamate receptor antagonism selectively modulates regional connectivity

Dopamine receptors in the NAc play a role in regulating activity in both glutamatergic and dopaminergic afferent and efferent projections (David et al., 2005; West et al., 2003). We showed that dopamine receptor antagonism decreased BOLD changes in HP and the AM.

Dopamine receptors within the NAc have previously been shown to play an integral role in memory consolidation and retrieval (Manago et al., 2009; Setlow, 1997). Dopamine afferents to the HP arising in the VTA have been shown to play a modulatory role in HP activity (Bethus et al., 2010). It has also been shown that striatal activation, including the NAc, plays a role in HP-dependent memory formation, possibly by enhancing memory consolidation (Wittmann et al., 2005). Concurrent dopamine receptor activation in the NAc and AM has also been shown to play a critical role in memory consolidation (LaLumiere et al., 2005). Thus, these studies may explain the role of dopamine receptor activation in the NAc following fornix stimulation as a possible mechanism underlying fornix DBS improvement of cognition and memory in AD patients. We observed that glutamate receptor blockade in the NAc also significantly decreased BOLD changes in the HP and the AM. Glutamate receptor antagonism in the NAc has been previously shown to block hippocampal modulation of VTA cell population activity (Floresco et al., 2001), consistent with this finding. Glutamate receptor signaling in the AM, together with dopamine receptor signaling in the NAc has been shown to promote motivated behavior (Ramirez et al., 2015; Stuber et al., 2011). We showed cluster size decreases throughout corticolimbic and medial limbic circuit structures with dopamine and glutamate receptor antagonism compared to vehicle microinfusion. We also observed a similar BOLD decrease in the HP and the AM with fornix DBS following dopamine and glutamate receptor antagonism. Future studies examining the global circuit recruitment are necessary to determine the precise role of glutamate and dopamine receptors in the NAc following fornix stimulation. However, this study provides fundamental information regarding the global circuit effects and potential mechanism behind the observed clinical improvement in cognition and memory recall on AD patients receiving fornix DBS.

Conclusion

Our data suggest that clinical fornix DBS may increase neurotransmitter release and activation of neural activity in medial limbic and corticolimbic circuit structures, which may underlie the observed restoration in basal activity levels within dysregulated circuits. We used a swine model due to the large brain volume (∼160 g), which is comparable to the non-human primate (rhesus macaque: ∼100 g), and with a gyrencephalic cortex, it more closely represents human brain anatomy than do the brains of small animal models (Wakeman et al., 2006). Although there are inherent limitations of translating findings from healthy animals to human pathologic conditions, the global and local circuitry effects in this study are significant in understanding the functional connectivity and potential mechanisms underlying effective fornix DBS modulating pathological brain activity in AD patients. Our collective findings compliment previous reports of circuit connectivity between the medial and corticolimbic circuits and provide a foundation for multimodal functional organization studies of the global impact of local pharmacological manipulations. Our study indicates that fornix stimulation drives medial and corticolimbic circuit interactions in a functional loop, which is partially involving regulation of major excitatory input into and through the NAc.

Supplementary Material

Refer to Web version on PubMed Central for supplementary material.

Acknowledgments

Support for this work came from the National Institutes of Health (R01 NS 70872 awarded to KHL) and The Grainger Foundation. We thank Andrea McConico for her technical support and animal monitoring. We thank William Gibson and Paola Testini for their time and input to the manuscript. We thank the Center for Advanced Imaging Research at The Mayo Clinic for their support.

References

Adcock RA, Thangavel A, Whitfield-Gabrieli S, Knutson B, Gabrieli JD. Reward-motivated learning: mesolimbic activation precedes memory formation. Neuron. 2006; 50:507–517. [PubMed: 16675403]

Anderberg, MR. Cluster analysis for applications. Academic Press; New, York: 1973.

Arnold SE, Hyman BT, Flory J, Damasio AR, Van Hoesen GW. The topographical and neuroanatomical distribution of neurofibrillary tangles and neuritic plaques in the cerebral cortex of patients with Alzheimer's disease. Cereb Cortex. 1991; 1:103–116. [PubMed: 1822725]

Badre D, Lebrecht S, Pagliaccio D, Long NM, Scimeca JM. Ventral striatum and the evaluation of memory retrieval strategies. Journal of cognitive neuroscience. 2014; 26:1928–1948. [PubMed: 24564466]

Benabid AL. Deep brain stimulation for Parkinson's disease. Current opinion in neurobiology. 2003; 13:696–706. [PubMed: 14662371]

Benabid AL, Pollak P, Gervason C, Hoffmann D, Gao DM, Hommel M, Perret JE, de Rougemont J. Long-term suppression of tremor by chronic stimulation of the ventral intermediate thalamic nucleus. Lancet. 1991; 337:403–406. [PubMed: 1671433]

Berke JD, Hyman SE. Addiction, dopamine, and the molecular mechanisms of memory. Neuron. 2000; 25:515–532. [PubMed: 10774721]

Bethus I, Tse D, Morris RG. Dopamine and memory: modulation of the persistence of memory for novel hippocampal NMDA receptor-dependent paired associates. The Journal of neuroscience. 2010; 30:1610–1618. [PubMed: 20130171]

Blaha CD, Yang CR, Floresco SB, Barr AM, Phillips AG. Stimulation of the ventral subiculum of the hippocampus evokes glutamate receptor-mediated changes in dopamine efflux in the rat nucleus accumbens. The European journal of neuroscience. 1997; 9:902–911. [PubMed: 9182943]

Bledsoe JM, Kimble CJ, Covey DP, Blaha CD, Agnesi F, Mohseni P, Whitlock S, Johnson DM, Horne A, Bennet KE, Lee KH, Garris PA. Development of the Wireless Instantaneous Neurotransmitter Concentration System for intraoperative neurochemical monitoring using fast-scan cyclic voltammetry. Journal of neurosurgery. 2009; 111:712–723. [PubMed: 19425890]

Boeijinga PH, Mulder AB, Pennartz CM, Manshanden I, Lopes da Silva FH. Responses of the nucleus accumbens following fornix/fimbria stimulation in the rat. Identification and long-term potentiation of mono- and polysynaptic pathways. Neuroscience. 1993; 53:1049–1058. [PubMed: 8389427]

Boeijinga PH, Pennartz CM, Lopes da Silva FH. Paired-pulse facilitation in the nucleus accumbens following stimulation of subicular inputs in the rat. Neuroscience. 1990; 35:301–311. [PubMed: 2381511]

Bressler SL, Menon V. Large-scale brain networks in cognition: emerging methods and principles. Trends in cognitive sciences. 2010; 14:277–290. [PubMed: 20493761]

Buckner RL, Snyder AZ, Shannon BJ, LaRossa G, Sachs R, Fotenos AF, Sheline YI, Klunk WE, Mathis CA, Morris JC, Mintun MA. Molecular, structural, and functional characterization of Alzheimer's disease: evidence for a relationship between default activity, amyloid, and memory. The Journal of neuroscience. 2005; 25:7709–7717. [PubMed: 16120771]

Carr MF, Jadhav SP, Frank LM. Hippocampal replay in the awake state: a potential substrate for memory consolidation and retrieval. Nature neuroscience. 2011; 14:147–153. [PubMed: 21270783]

Chang SY, Kim I, Marsh MP, Jang DP, Hwang SC, Van Gompel JJ, Goerss SJ, Kimble CJ, Bennet KE, Garris PA, Blaha CD, Lee KH. Wireless fast-scan cyclic voltammetry to monitor adenosine in

patients with essential tremor during deep brain stimulation. Mayo Clinic proceedings Mayo Clinic. 2012; 87:760–765.

Cho ZH, Min HK, Oh SH, Han JY, Park CW, Chi JG, Kim YB, Paek SH, Lozano AM, Lee KH. Direct visualization of deep brain stimulation targets in Parkinson disease with the use of 7-tesla magnetic resonance imaging. Journal of neurosurgery. 2010; 113:639–647. [PubMed: 20380532]

David HN, Ansseau M, Abraini JH. Dopamine-glutamate reciprocal modulation of release and motor responses in the rat caudate-putamen and nucleus accumbens of “intact” animals. Brain research Brain research reviews. 2005; 50:336–360. [PubMed: 16278019]

Day JJ, Roitman MF, Wightman RM, Carelli RM. Associative learning mediates dynamic shifts in dopamine signaling in the nucleus accumbens. Nature neuroscience. 2007; 10:1020–1028. [PubMed: 17603481]

Dunteman, GH. Principal Components Analysis. SAGE Publishing; 1989.

Felix B, Leger ME, Albe-Fessard D, Marcilloux JC, Rampin O, Laplace JP. Stereotaxic atlas of the pig brain. Brain research bulletin. 1999; 49:1–137. [PubMed: 10466025]

Ferretti V, Florian C, Costantini VJ, Roullet P, Rinaldi A, De Leonibus E, Oliverio A, Mele A. Co-activation of glutamate and dopamine receptors within the nucleus accumbens is required for spatial memory consolidation in mice. Psychopharmacology. 2005; 179:108–116. [PubMed: 15682297]

Flagel SB, Clark JJ, Robinson TE, Mayo L, Czuj A, Willuhn I, Akers CA, Clinton SM, Phillips PE, Akil H. A selective role for dopamine in stimulus-reward learning. Nature. 2011; 469:53–57. [PubMed: 21150898]

Floresco SB, Todd CL, Grace AA. Glutamatergic afferents from the hippocampus to the nucleus accumbens regulate activity of ventral tegmental area dopamine neurons. The Journal of neuroscience. 2001; 21:4915–4922. [PubMed: 11425919]

Floresco SB, West AR, Ash B, Moore H, Grace AA. Afferent modulation of dopamine neuron firing differentially regulates tonic and phasic dopamine transmission. Nature neuroscience. 2003; 6:968–973. [PubMed: 12897785]

Floresco SB. The nucleus accumbens: an interface between cognition, emotion, and action. Annual review of psychology. 2015; 66:25–52.

Friedman DP, Aggleton JP, Saunders RC. Comparison of hippocampal, amygdala, and perirhinal projections to the nucleus accumbens: combined anterograde and retrograde tracing study in the Macaque brain. The Journal of comparative neurology. 2002; 450:345–365. [PubMed: 12209848]

Geula C. Abnormalities of neural circuitry in Alzheimer's disease: hippocampus and cortical cholinergic innervation. Neurology. 1998; 51:S18–29. discussion S65-17. [PubMed: 9674759]

Goto Y, Grace AA. Limbic and cortical information processing in the nucleus accumbens. Trends in neurosciences. 2008; 31:552–558. [PubMed: 18786735]

Greene P. Deep-brain stimulation for generalized dystonia. The New England journal of medicine. 2005; 352:498–500. [PubMed: 15689590]

Greicius MD, Srivastava G, Reiss AL, Menon V. Default-mode network activity distinguishes Alzheimer's disease from healthy aging: evidence from functional MRI. Proceedings of the National Academy of Sciences of the United States of America. 2004; 101:4637–4642. [PubMed: 15070770]

Hamann SB, Ely TD, Grafton ST, Kilts CD. Amygdala activity related to enhanced memory for pleasant and aversive stimuli. Nature neuroscience. 1999; 2:289–293. [PubMed: 10195224]

Hardenacke K, Shubina E, Buhrle CP, Zapf A, Lenartz D, Klosterkotter J, Visser-Vandewalle V, Kuhn J. Deep brain stimulation as a tool for improving cognitive functioning in Alzheimer's dementia: a systematic review. Frontiers in psychiatry. 2013; 4:159. [PubMed: 24363647]

Helbing C, Werner G, Angenstein F. Variations in the temporal pattern of perforant pathway stimulation control the activity in the mesolimbic pathway. NeuroImage. 2013; 64:43–60. [PubMed: 22982727]

Hescham S, Lim LW, Jahanshahi A, Steinbusch HW, Prickaerts J, Blokland A, Temel Y. Deep brain stimulation of the forniceal area enhances memory functions in experimental dementia: the role of stimulation parameters. Brain Stimul. 2013; 6:72–77. [PubMed: 22405739]

Horner AJ, Bisby JA, Bush D, Lin WJ, Burgess N. Evidence for holistic episodic recollection via hippocampal pattern completion. Nature communications. 2015; 6:7462.

Hyman BT, Van Hoesen GW, Damasio AR, Barnes CL. Alzheimer's disease: cell-specific pathology isolates the hippocampal formation. Science. 1984; 225:1168–1170. [PubMed: 6474172]

Kahn I, Shohamy D. Intrinsic connectivity between the hippocampus, nucleus accumbens, and ventral tegmental area in humans. Hippocampus. 2013; 23:187–192. [PubMed: 23129267]

Kawaguchi K, Simon RP. Deep prepiriform cortex modulates neuronal cell death in global ischemia. Journal of cerebral blood flow and metabolism : official journal of the International Society of Cerebral Blood Flow and Metabolism. 1997; 17:356–360.

Kelley AE. Memory and addiction: shared neural circuitry and molecular mechanisms. Neuron. 2004; 44:161–179. [PubMed: 15450168]

Kelley AE, Domesick VB. The distribution of the projection from the hippocampal formation to the nucleus accumbens in the rat: an anterograde- and retrograde-horseradish peroxidase study. Neuroscience. 1982; 7:2321–2335. [PubMed: 6817161]

Kim JP, Min HK, Knight EJ, Duffy PS, Abulseoud OA, Marsh MP, Kelsey K, Blaha CD, Bennet KE, Frye MA, Lee KH. Centromedian-parafascicular deep brain stimulation induces differential functional inhibition of the motor, associative, and limbic circuits in large animals. Biological psychiatry. 2013; 74:917–926. [PubMed: 23993641]

Knight EJ, Testini P, Min HK, Gibson WS, Gorny KR, Favazza CP, Felmlee JP, Kim I, Welker KM, Clayton DA, Kassen BT, Chang SY, Lee KH. Motor and Nonmotor Circuitry Activation Induced by Subthalamic Nucleus Deep Brain Stimulation in Patients With Parkinson Disease: Intraoperative Functional Magnetic Resonance Imaging for Deep Brain Stimulation. Mayo Clinic proceedings. 2015; 90:773–785. [PubMed: 26046412]

Knutson B, Gibbs SE. Linking nucleus accumbens dopamine and blood oxygenation. Psychopharmacology. 2007; 191:813–822. [PubMed: 17279377]

Krautwald K, Min HK, Lee KH, Angenstein F. Synchronized electrical stimulation of the rat medial forebrain bundle and perforant pathway generates an additive BOLD response in the nucleus accumbens and prefrontal cortex. NeuroImage. 2013; 77:14–25. [PubMed: 23558098]

Krimer LS, Muly EC 3rd, Williams GV, Goldman-Rakic PS. Dopaminergic regulation of cerebral cortical microcirculation. Nature neuroscience. 1998; 1:286–289. [PubMed: 10195161]

LaLumiere RT, Nawar EM, McGaugh JL. Modulation of memory consolidation by the basolateral amygdala or nucleus accumbens shell requires concurrent dopamine receptor activation in both brain regions. Learn Mem. 2005; 12:296–301. [PubMed: 15930508]

Laxton AW, Lozano AM. Deep brain stimulation for the treatment of Alzheimer disease and dementias. World neurosurgery. 2013; 80:S28 e21–28. [PubMed: 22722036]

Laxton AW, Tang-Wai DF, McAndrews MP, Zumsteg D, Wennberg R, Keren R, Wherrett J, Naglie G, Hamani C, Smith GS, Lozano AM. A phase I trial of deep brain stimulation of memory circuits in Alzheimer's disease. Annals of neurology. 2010; 68:521–534. [PubMed: 20687206]

Lee H, Fell J, Axmacher N. Electrical engram: how deep brain stimulation affects memory. Trends in cognitive sciences. 2013; 17:574–584. [PubMed: 24126128]

Legault M, Rompre PP, Wise RA. Chemical stimulation of the ventral hippocampus elevates nucleus accumbens dopamine by activating dopaminergic neurons of the ventral tegmental area. The Journal of neuroscience : the official journal of the Society for Neuroscience. 2000; 20:1635–1642. [PubMed: 10662853]

Lisman J, Grace AA, Duzel E. A neoHebbian framework for episodic memory; role of dopamine-dependent late LTP. Trends in neurosciences. 2011; 34:536–547. [PubMed: 21851992]

Lisman JE, Grace AA. The hippocampal-VTA loop: controlling the entry of information into long-term memory. Neuron. 2005; 46:703–713. [PubMed: 15924857]

Lopes da Silva FH, Arnolds DE, Neijt HC. A functional link between the limbic cortex and ventral striatum: physiology of the subiculum accumbens pathway. Experimental brain research. 1984; 55:205–214. [PubMed: 6745361]

Lozano AM, Giacobbe P, Hamani C, Rizvi SJ, Kennedy SH, Kolivakis TT, Debonnel G, Sadikot AF, Lam RW, Howard AK, Ilcewicz-Klimek M, Honey CR, Mayberg HS. A multicenter pilot study of

subcallosal cingulate area deep brain stimulation for treatment-resistant depression. Journal of neurosurgery. 2012; 116:315–322. [PubMed: 22098195]

Luo AH, Tahsili-Fahadan P, Wise RA, Lupica CR, Aston-Jones G. Linking context with reward: a functional circuit from hippocampal CA3 to ventral tegmental area. Science. 2011; 333:353–357. [PubMed: 21764750]

Luthi A, Luscher C. Pathological circuit function underlying addiction and anxiety disorders. Nature neuroscience. 2014; 17:1635–1643. [PubMed: 25402855]

Maguire EA, Frith CD. Aging affects the engagement of the hippocampus during autobiographical memory retrieval. Brain : a journal of neurology. 2003; 126:1511–1523. [PubMed: 12805116]

Manago F, Castellano C, Oliverio A, Mele A, De Leonibus E. Role of dopamine receptors subtypes, D1-like and D2-like, within the nucleus accumbens subregions, core and shell, on memory consolidation in the one-trial inhibitory avoidance task. Learn Mem. 2009; 16:46–52. [PubMed: 19117916]

Mardia, KV.; Kent, JT.; Bibby, JM. Multivariate Analysis (Probability and Mathematical Statistics). Academic Press; 1980.

McIntosh AR. Mapping cognition to the brain through neural interactions. Memory. 1999; 7:523–548. [PubMed: 10659085]

McIntyre CC, Hahn PJ. Network perspectives on the mechanisms of deep brain stimulation. Neurobiology of disease. 2010; 38:329–337. [PubMed: 19804831]

Mesulam MM. A plasticity-based theory of the pathogenesis of Alzheimer's disease. Annals of the New York Academy of Sciences. 2000; 924:42–52. [PubMed: 11193801]

Min HK, Ross EK, Lee KH, Dennis K, Han SR, Jeong JH, Marsh MP, Striemer B, Felmlee JP, Luis Lujan J, Goerss S, Duffy PS, Blaha CD, Chang SY, Bennet KE. Subthalamic nucleus deep brain stimulation induces motor network BOLD activation: Use of a high precision MRI guided stereotactic system for nonhuman primates. Brain stimulation. 2014; 7:603–607. [PubMed: 24933029]

Min HK, Hwang SC, Marsh MP, Kim I, Knight E, Striemer B, Felmlee JP, Welker KM, Blaha CD, Chang SY, Bennet KE, Lee KH. Deep brain stimulation induces BOLD activation in motor and non-motor networks: an fMRI comparison study of STN and EN/GPi DBS in large animals. NeuroImage. 2012; 63:1408–1420. [PubMed: 22967832]

Nestor PJ, Fryer TD, Hodges JR. Declarative memory impairments in Alzheimer's disease and semantic dementia. NeuroImage. 2006; 30:1010–1020. [PubMed: 16300967]

O'Donnell P, Grace AA. Synaptic interactions among excitatory afferents to nucleus accumbens neurons: hippocampal gating of prefrontal cortical input. The Journal of neuroscience. 1995; 15:3622–3639. [PubMed: 7751934]

Okun MS. Deep-brain stimulation--entering the era of human neural-network modulation. The New England journal of medicine. 2014; 371:1369–1373. [PubMed: 25197963]

Pennartz CM, Ito R, Verschure PF, Battaglia FP, Robbins TW. The hippocampal-striatal axis in learning, prediction and goal-directed behavior. Trends in neurosciences. 2011; 34:548–559. [PubMed: 21889806]

Ponce FA, Asaad W, Foote KD, Anderson WS, Cosgrove R, Baltuch GH, Beasley KD, Reymers DE, Oh ES, Targum SD, Smith G, Lyketsos CG, Lozano AM. 130 Bilateral Fornix Deep Brain Stimulation for Alzheimer Disease: Surgical Safety in the ADvance Trial. Neurosurgery 62 Suppl 1, Clinical neurosurgery. 2015; 207

Rajmohan V, Mohandas E. The limbic system. Indian journal of psychiatry. 2007; 49:132–139. [PubMed: 20711399]

Ramirez F, Moscarello JM, LeDoux JE, Sears RM. Active avoidance requires a serial basal amygdala to nucleus accumbens shell circuit. The Journal of neuroscience. 2015; 35:3470–3477. [PubMed: 25716846]

Reyes PF, Golden GT, Fagel PL, Fariello RG, Katz L, Carner E. THe prepiriform cortex in dementia of the alzheimer type. Archives of Neurology. 1987; 44:644–645. [PubMed: 3579682]

Rossato JI, Bevilaqua LR, Izquierdo I, Medina JH, Cammarota M. Dopamine controls persistence of long-term memory storage. Science. 2009; 325:1017–1020. [PubMed: 19696353]

Saikali S, Meurice P, Sauleau P, Eliat PA, Bellaud P, Randuineau G, Verin M, Malbert CH. A three-dimensional digital segmented and deformable brain atlas of the domestic pig. Journal of neuroscience methods. 2010; 192:102–109. [PubMed: 20692291]

Saint Marie RL, Miller EJ, Breier MR, Weber M, Swerdlow NR. Projections from ventral hippocampus to medial prefrontal cortex but not nucleus accumbens remain functional after fornix lesions in rats. Neuroscience. 2010; 168:498–504. [PubMed: 20338222]

Sankar T, Chakravarty MM, Bescos A, Lara M, Obuchi T, Laxton AW, McAndrews MP, Tang-Wai DF, Workman CI, Smith GS, Lozano AM. Deep brain stimulation influences brain structure in Alzheimer's disease. Brain stimulation. 2014; 8:645–654. [PubMed: 25814404]

Saunders RC, Aggleton JP. Origin and topography of fibers contributing to the fornix in macaque monkeys. Hippocampus. 2007; 17:396–411. [PubMed: 17372974]

Schedlbauer AM, Copara MS, Watrous AJ, Ekstrom AD. Multiple interacting brain areas underlie successful spatiotemporal memory retrieval in humans. Scientific reports. 2014; 4:6431. [PubMed: 25234342]

Scimeca JM, Badre D. Striatal contributions to declarative memory retrieval. Neuron. 2012; 75:380–392. [PubMed: 22884322]

Selden N, Geula C, Hersh L, Mesulam MM. Human striatum: chemoarchitecture of the caudate nucleus, putamen and ventral striatum in health and Alzheimer's disease. Neuroscience. 1994; 60:621–636. [PubMed: 7523983]

Sesack SR, Grace AA. Cortico-basal ganglia reward network: microcircuitry. Neuropsychopharmacology : official publication of the American College of Neuropsychopharmacology. 2010; 35:27–47. [PubMed: 19675534]

Setlow B. The nucleus accumbens and learning and memory. Journal of neuroscience research. 1997; 49:515–521. [PubMed: 9302072]

Shohamy D, Adcock RA. Dopamine and adaptive memory. Trends in cognitive sciences. 2010; 14:464–472. [PubMed: 20829095]

Shon YM, Chang SY, Tye SJ, Kimble CJ, Bennet KE, Blaha CD, Lee KH. Comonitoring of adenosine and dopamine using the Wireless Instantaneous Neurotransmitter Concentration System: proof of principle. Journal of neurosurgery. 2010; 112:539–548. [PubMed: 19731995]

Smith GS, Laxton AW, Tang-Wai DF, McAndrews MP, Diaconescu AO, Workman CI, Lozano AM. Increased cerebral metabolism after 1 year of deep brain stimulation in Alzheimer disease. Arch Neurol. 2012; 69:1141–1148. [PubMed: 22566505]

Smith SM, Jenkinson M, Woolrich MW, Beckmann CF, Behrens TE, Johansen-Berg H, Bannister PR, De Luca M, Drobnjak I, Flitney DE, Niazy RK, Saunders J, Vickers J, Zhang Y, De Stefano N, Brady JM, Matthews PM. Advances in functional and structural MR image analysis and implementation as FSL. NeuroImage. 2004; 23 Suppl 1:S208–219. [PubMed: 15501092]

Speer ME, Bhanji JP, Delgado MR. Savoring the past: positive memories evoke value representations in the striatum. Neuron. 2014; 84:847–856. [PubMed: 25451197]

Sporns O. Contributions and challenges for network models in cognitive neuroscience. Nature neuroscience. 2014; 17:652–660. [PubMed: 24686784]

Squire LR. Memory and the hippocampus: a synthesis from findings with rats, monkeys, and humans. Psychological review. 1992; 99:195–231. [PubMed: 1594723]

Squire LR. Memory systems of the brain: a brief history and current perspective. Neurobiology of learning and memory. 2004; 82:171–177. [PubMed: 15464402]

Starr PA, Christine CW, Theodosopoulos PV, Lindsey N, Byrd D, Mosley A, Marks WJ Jr. Implantation of deep brain stimulators into the subthalamic nucleus: technical approach and magnetic resonance imaging-verified lead locations. Journal of neurosurgery. 2002; 97:370–387. [PubMed: 12186466]

Stuber GD, Hnasko TS, Britt JP, Edwards RH, Bonci A. Dopaminergic terminals in the nucleus accumbens but not the dorsal striatum corelease glutamate. The Journal of neuroscience. 2010; 30:8229–8233. [PubMed: 20554874]

Stuber GD, Sparta DR, Stamatakis AM, van Leeuwen WA, Hardjoprajitno JE, Cho S, Tye KM, Kempadoo KA, Zhang F, Deisseroth K, Bonci A. Excitatory transmission from the amygdala to nucleus accumbens facilitates reward seeking. Nature. 2011; 475:377–380. [PubMed: 21716290]

Suthana N, Haneef Z, Stern J, Mukamel R, Behnke E, Knowlton B, Fried I. Memory enhancement and deep-brain stimulation of the entorhinal area. The New England journal of medicine. 2012; 366:502–510. [PubMed: 22316444]

Totterdell S, Smith AD. Convergence of hippocampal and dopaminergic input onto identified neurons in the nucleus accumbens of the rat. Journal of chemical neuroanatomy. 1989; 2:285–298. [PubMed: 2572241]

Tsivilis D, Vann SD, Denby C, Roberts N, Mayes AR, Montaldi D, Aggleton JP. A disproportionate role for the fornix and mammillary bodies in recall versus recognition memory. Nature neuroscience. 2008; 11:834–842. [PubMed: 18552840]

Valenti O, Lodge DJ, Grace AA. Aversive stimuli alter ventral tegmental area dopamine neuron activity via a common action in the ventral hippocampus. The Journal of neuroscience. 2011; 31:4280–4289. [PubMed: 21411669]

Vann SD, Tsivilis D, Denby CE, Quamme JR, Yonelinas AP, Aggleton JP, Montaldi D, Mayes AR. Impaired recollection but spared familiarity in patients with extended hippocampal system damage revealed by 3 convergent methods. Proceedings of the National Academy of Sciences of the United States of America. 2009; 106:5442–5447. [PubMed: 19289844]

Wakeman DR, Crain AM, Snyder EY. Large animal models are critical for rationally advancing regenerative therapies. Regen Med. 2006; 1:405–413. [PubMed: 17465832]

West AR, Floresco SB, Charara A, Rosenkranz JA, Grace AA. Electrophysiological interactions between striatal glutamatergic and dopaminergic systems. Annals of the New York Academy of Sciences. 2003; 1003:53–74. [PubMed: 14684435]

Wilson CR, Baxter MG, Easton A, Gaffan D. Addition of fornix transection to frontal-temporal disconnection increases the impairment in object-in-place memory in macaque monkeys. The European journal of neuroscience. 2008; 27:1814–1822. [PubMed: 18380673]

Wittmann BC, Schott BH, Guderian S, Frey JU, Heinze HJ, Duzel E. Reward-related FMRI activation of dopaminergic midbrain is associated with enhanced hippocampus-dependent long-term memory formation. Neuron. 2005; 45:459–467. [PubMed: 15694331]

Yang CR, Mogenson GJ. Electrophysiological responses of neurones in the nucleus accumbens to hippocampal stimulation and the attenuation of the excitatory responses by the mesolimbic dopaminergic system. Brain research. 1984; 324:69–84. [PubMed: 6151418]

Yang CR, Mogenson GJ. An electrophysiological study of the neural projections from the hippocampus to the ventral pallidum and the subpallidal areas by way of the nucleus accumbens. Neuroscience. 1985; 15:1015–1024. [PubMed: 4047397]

Zaldivar D, Rauch A, Whittingstall K, Logothetis NK, Goense J. Dopamine-induced dissociation of BOLD and neural activity in macaque visual cortex. Current biology : CB. 2014; 24:2805–2811. [PubMed: 25456449]

Zhang S, Qi J, Li X, Wang HL, Britt JP, Hoffman AF, Bonci A, Lupica CR, Morales M. Dopaminergic and glutamatergic microdomains in a subset of rodent mesoaccumbens axons. Nature neuroscience. 2015; 18:386–392. [PubMed: 25664911]

Zhou J, Seeley WW. Network dysfunction in Alzheimer's disease and frontotemporal dementia: implications for psychiatry. Biological psychiatry. 2014; 75:565–573. [PubMed: 24629669]

Highlights

- Fornix deep brain stimulation results in hemodynamic increases in medial limbic and corticolimbic circuit structures
- Fornix deep brain stimulation results in triphasic dopamine release in the nucleus accumbens
- Fornix deep brain stimulation-induced hemodynamic increases in the hippocampus and amygdala are at least partially dependent on circuit involvement via the nucleus accumbens

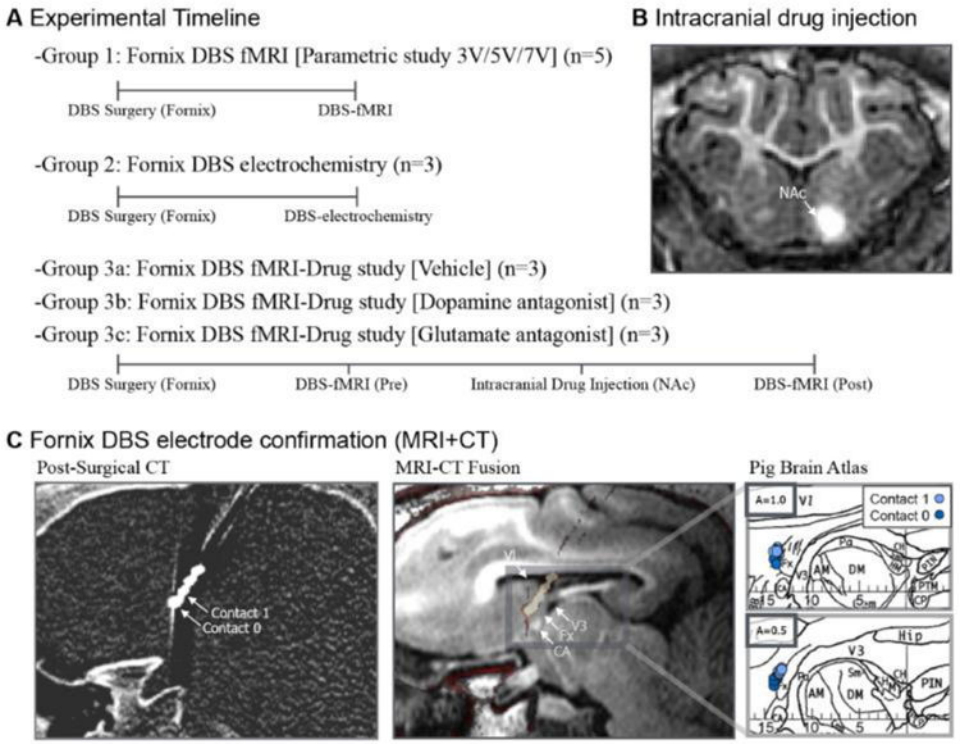

Figure 1.

Experimental setup and DBS electrode target confirmation. (A) Experimental timeline of the three distinct experimental paradigms. (B) Contrast agent intracranial microinjection into NAc for drug injection target and diffusion confirmation. (C) CT-based DBS electrode target confirmation pre-surgical MRI and post-surgical CT showing the electrode contacts 0, and 1. Anatomical confirmation of the DBS lead for each subject marked on the axial plane of the swine atlas (reprinted from (Felix et al., 1999) with permission from Elsevier, copyright 1999). Abbreviations: AM, medial anterior thalamic nucleus; CA, anterior commissure; CH, habenular commissure; CP, posterior commissure; DM dorsal medial thalamic nucleus; Fx, Fornix; Hip, Hippocampus; HM, medial habenular nucleus; PTM, medial pretectal nucleus; V1, first ventricle; V3, third ventricle.

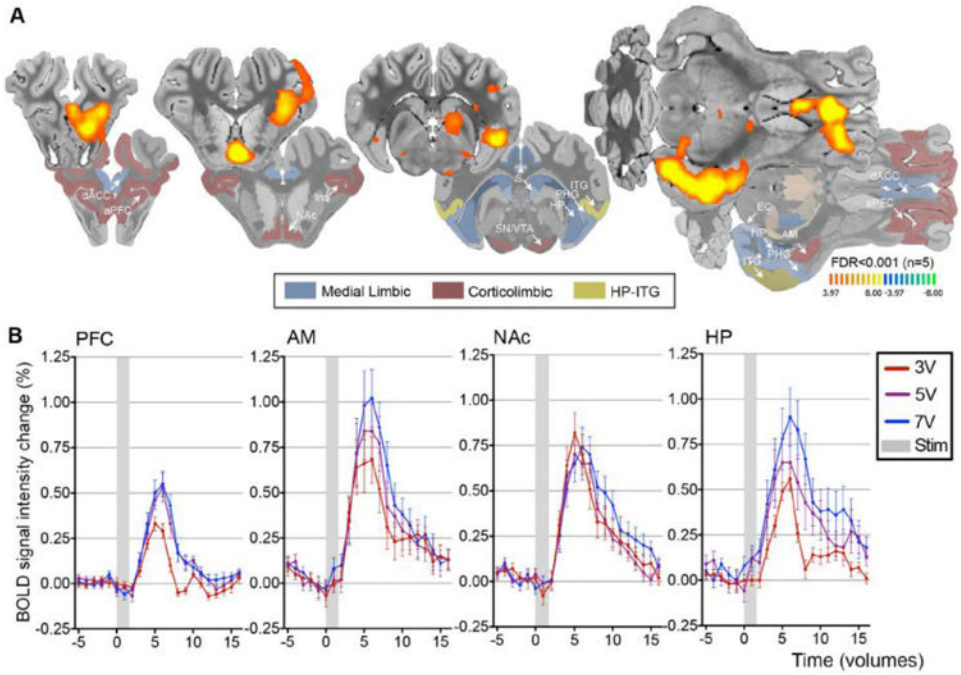

Figure 2.

fMRI BOLD effects following fornix stimulation. (A) Fornix DBS-evoked positive BOLD responses in medial limbic and corticolimbic structures (3 V, 130 Hz, 150 μsec pulse width). (B) BOLD signal intensity change (%) following fornix DBS. The representative BOLD signal intensity change (y axis) for all subjects (n=5), five stimulation blocks averaged in each volume of interest. Abbreviations: AM, amygdala; BOLD, blood oxygenation-level dependent; dACC, dorsal anterior cingulate cortex; EC, entorhinal cortex; Ins, Insular cortex; DBS, deep brain stimulation; HP, hippocampus; PHG, parahippocampus; ITG, inferior temporal gyrus; NAc, nucleus accumbens; S, septum; SN/VTA, substantia nigra/ ventral tegmental area; aPFC, anterior prefrontal cortex; Stim, stimulation.

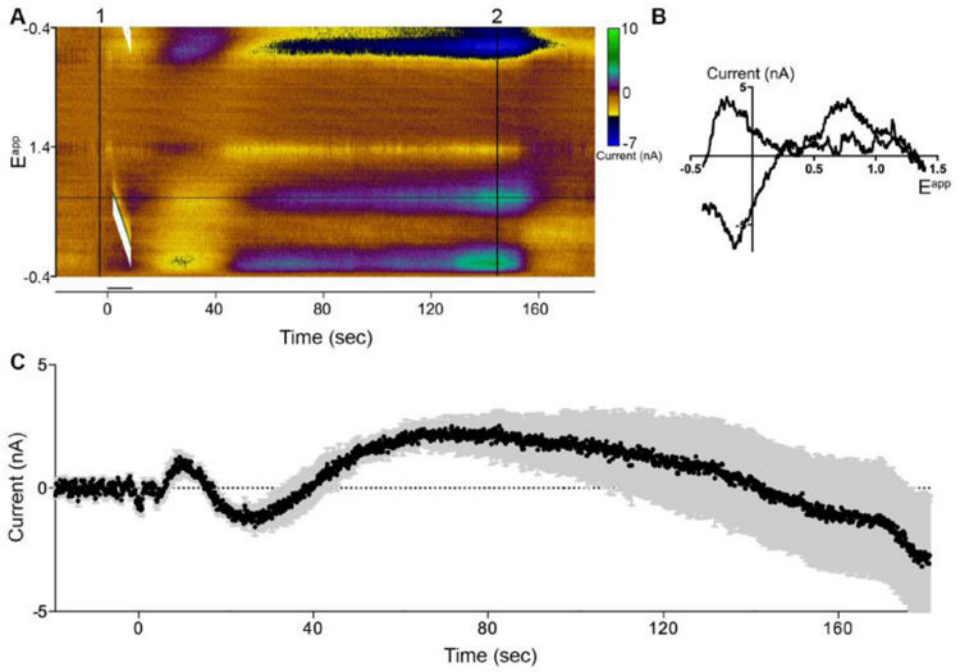

Figure 3.

Fornix DBS (3 V, 130 Hz, 150 μsec) evoked DA release in the NAc. (A) Fornix DBS results in biphasic DA release. Representative three-dimensional color plot from a single subject shows stimulation (6 sec) time-locked and latent DA response. Background subtraction (1). (B) Representative cyclic voltammogram depicted from color plot (2). (C) Current versus time plot at +0.6 V showing DA (black line) release following electrical stimulation ±SEM (grey bars) (n=3, 2 samples per subject).

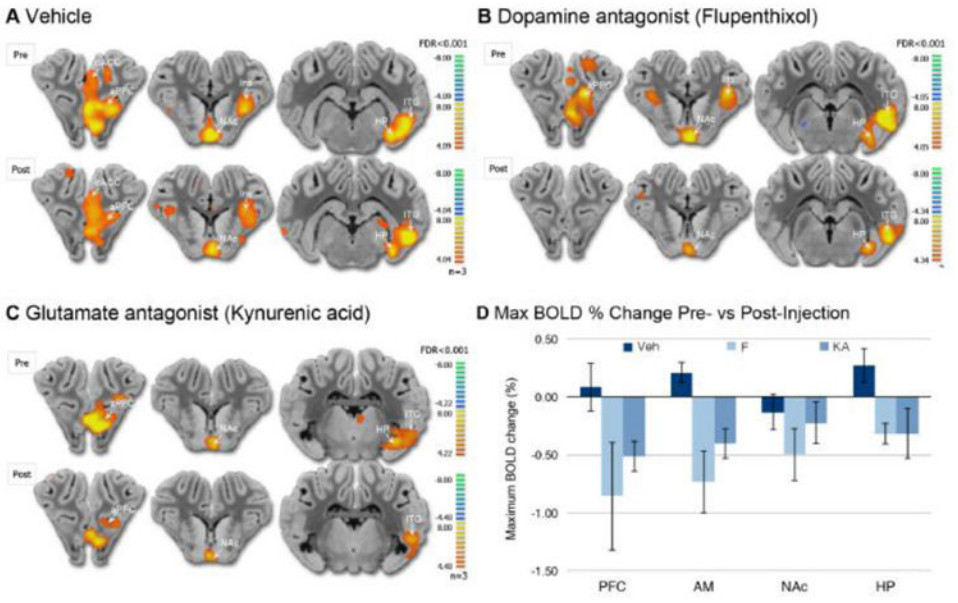

Figure 4.

fMRI BOLD changes following intracranial drug microinfusion in NAc. (A) Representative brain atlas slice showing stimulation-induced BOLD response pre- and post-vehicle microinfusion (3 V, 130Hz, 150 μsec). (B) Representative brain atlas slice showing BOLD response pre- and post- flupenthixol microinfusion. (C) Representative brain atlas slice showing BOLD response pre- and post-kynurenic acid microinfusion. (D) The peak BOLD % change pre- and post-drug microinfusion of vehicle, kynurenic acid as a general ionotropic glutamate receptor antagonist, or flupenthixol microinfusion as a general D1/D2 receptor antagonist (n=3 per treatment group). Abbreviations: Abbreviations: AM, amygdala; aPFC, anterior prefrontal cortex; dACC, dorsal anterior cingulate cortex; HP, hippocampus; Ins, insular cortex; ITG, inferior temporal gyrus; NAc, nucleus accumbens; Veh, vehicle; KA, kynurenic acid; Flu, α-flupenthixol.

Table 1

Brain areas of significant BOLD response

Location	Circuit Involvement	Cluster Size (mm^3)			Coordinates (x,y,z)	Max t-score		
		3 V	5 V	7 V		3 V	5 V	7 V
Nucleus accumbens (I)	A	588	1118	1366	-1.5, 20.6, -4.6	**13.83***	**15.35***	**13.68***
Anterior prefrontal cortex (I)	A	1217	1934	3110	-4.1, 32.9, 0.6	**13.61***	**13.22***	**15.78***
Dorsal anterior cingulate (I)	A/B	656	1059	1512	-1.6, 30.6, 3.8	**12.98***	**15.35***	**14.54***
Inferior temporal gyrus (I)	C	468	1038	1617	-20.5, 0.9, 3.2	**9.20***	**15.74***	**15.11***
Hippocampus (I)	B	909	1012	1019	-13.0, -4.4, 4.4	**9.20***	**10.52***	**13.23***
Anterior hypothalamus (I)	D	180	427	395	-1.1, 12.1, -3.2	**9.14***	**10.21***	**9.48***
Parahippocampal gyrus (I)	B	430	1473	2084	-16.8, -5.4, 2.5	**8.70***	**12.85***	**13.18***
Entorhinal cortex (I)	B	370	434	489	-14.8, -3.6, 0.6	**8.35***	**8.35***	**8.16***
Insular cortex (I)	A	1104	3101	3975	-12.1, 29.4, 7.1	**8.30***	**15.11***	**17.16***
Amygdala (I)	A	685	930	943	-16.5, 6.9, -2.8	**8.16***	**13.21***	**13.18***
Fornix (I)	B	106	181	350	-2.7, 8.4, 9.1	**6.65***	**8.55***	**8.16***
Mammillary body (I)	B		119	168	-1.1, 4.6, -7.8		**9.41***	**6.80***
Parahippocampal gyrus (C)	B		154	190	12.2, -9.1, 4.6		5.45	**5.70***
Anterior thalamic nucleus (I)	B		448	341	-4.1, 3.4, -2.5		**10.69***	**7.18***
Prepyriform (I)	E		522	507	-16.5, 10.9, -0.8		**9.06***	**10.43***
Fornix (C)	B		325	364	1.1, 7.4, 10.2		**8.93***	**8.32***
Primary somatosensory cortex (I)	F		1242	1268	-13.9, 15.6, 17.0		**7.64***	**10.08***
Dorsolateral prefrontal cortex (I)	A		234	685	-6.3, 27.4, 11.1		**7.66***	**10.05***
Substantia nigra/VTA (I)	A		340	166	-8.3, -1.1, -6.1		**6.12***	**5.98***
Dorsal posterior cingulate (C)	B		1154	177	1.4, -7.4, 18.9		5.93	5.21
Periaqueductal gray (I)	G		277		-2.3, -6.6, -3.2		5.86	
Hippocampus (C)	B		235	851	11.5, -6.9, 8.9		5.32	**6.00***
Substantia nigra (C)	A		122		8.3, -0.9, -6.0		5.27	

Location	Circuit Involvement	Cluster Size (mm^3)			Coordinates (x,y,z)	Max t-score		
		3 V	5 V	7 V		3 V	5 V	7 V
Insular cortex (C)	A			774	19.4, 12.4, 9.6			**6.76***
Primary somatosensory cortex (C)	F			196	13.7, 14.4, 22.7			**6.45***
Entorhinal cortex (C)	B			280	2.6, -5.4, 7.2			5.82
Dorsal posterior cingulate (I)	B			126	-1.0, -9.6, 18.9			**5.66***
Dorsolateral cingulate (C)	B			118	9.2, 24.6, 3.4			5.63

*Areas showing with Bonferroni correction ($p<0.001$)

Circuit Involvement: A=corticolimbic; B=medial limbic; C= HC-ITG; D=HC-hypothalamus; E=HC-prepyriform; F= HC-PSC; G=NAc-PAG. Coordinates (mm): x=mediolateral, y=rostrocaudal, and z=dorsoventral. Abbreviations: C, Contralateral; I, Ipsilateral; VTA, ventral tegmental area; HC, hippocampus; NAc, nucleus accumbens; ITG, inferior temporal gyrus; PSC, primary somatosensory cortex; PAG, periaqueductal gray.

Table 2

Brain areas of significant BOLD response following NAc drug infusion

	Location	Circuit Involvement	Cluster Size (mm^3)		Coordinates (x,y,z)	Max t-score	
			Pre	Post		Pre	Post
Vehicle	Nucleus accumbens (I)	A	507	611	-2.6, 21.5, -5.3	**13.72***	**11.68***
	Anterior prefrontal cortex (I)	A	1351	1048	-4.2, 33.3, -4.7	**12.65***	**10.78***
	Dorsal anterior cingulate (I)	A/B	545	476	-1.0, 32.3, 3.62	**11.76***	**9.88***
	Insular cortex (I)	A	782	912	-12.5, 32.6, 3.0	**9.27***	**7.41***
	Hippocampus (I)	B	576	564	-16.2, 0.9, -2.7	**9.07***	**8.92***
	Inferior temporal gyrus (I)	C	475	783	-20.7, 0.9, 3.0	**9.07***	**12.87***
	Parahippocampal gyrus (I)	B	544	466	-17.3, -3.4, -2.6	**7.96***	**6.83***
	Amygdala (I)	A	446	596	-15.9, 6.9, -3.5	**7.63***	**9.33***
Flupenthixol	Nucleus accumbens (I)	A	488	103	-1.1, 19.4, -4.3	**10.28***	**10.28***
	Anterior prefrontal cortex (I)	A	1076		-5.6, 36.1, 3.5	**9.41***	4.58
	Dorsal anterior cingulate (I)	A/B	536	120	-1.3, 25.6, 7.0	**12.76***	**12.76***
	Insular cortex (I)	A	780		-16.5, 14.9, 11.9	**9.94***	
	Hippocampus (I)	B	505	285	-13.0, -2.4, 8.3	**11.44***	**8.51***
	Inferior temporal gyrus (I)	C	1055	483	-21.8, -3.9, 2.7	**11.86***	**11.86***
	Parahippocampal gyrus (I)	B	771	425	-13.8, -7.9, 3.8	**11.77***	**11.77***
	Amygdala (I)	A	462	245	-16.7, 4.9, 1.3	**9.40***	**8.54***
	Entorhinal cortex (I)	B	126		-4.3, -2.4, 8.3	**7.20***	3.05
Kynurenic Acid	Nucleus accumbens (I)	A	481	100	-2.6, 22.6, -5.3	**8.82***	**8.26***
	Anterior prefrontal cortex (I)	A	1058	635	-4.2, 33.1, -4.8	**13.31***	**8.92***
	Dorsal anterior cingulate (I)	A/B	156		-1.0, 25.1, 6.6	**9.16***	
	Insular cortex (I)	A	387		-13.0, 29.1, 3.0	**6.85***	**5.80***
	Hippocampus (I)	B	251		-12.5, 1.9, -5.3	**9.34***	

Location	Circuit Involvement	Cluster Size (mm^3)		Coordinates (x,y,z)	Max t-score	
		Pre	Post		Pre	Post
Inferior temporal gyrus (I)	C	228	244	-19.2, 5.9, 4.5	**9.48***	**7.49***
Parahippocampal gyrus (I)	B	204		-14.8, -7.9, 0.2	**6.72***	4.91
Amygdala (I)	A	381		-16.4, 4.9, 0.3	**9.48***	5.74

* Areas showing with Bonferroni correction ($p<0.001$)

Circuit Involvement: A=corticolimbic; B=medial limbic; C= HC-ITG. Coordinates (mm): x=mediolateral, y=rostrocaudal, and z=dorsoventral. Abbreviations: I, Ipsilateral; HC, hippocampus; NAc, nucleus accumbens; ITG, inferior temporal gyrus.